Wear analysis of journal bearing coatings by atomic force microscopy

R. Bassani, E. Ciulli, M. Labardi, M. Allegrini

Wear phenomena occurring to journal bearing coatings, designed for extreme performance, are studied on the micro-nanometer scale by means of scanning probe microscopy, particularly the atomic force microscope in the friction force mode. A morphological as well as tribological investigation on the micro-nanometer scale has been carried out on bushes of different type, namely on electroplated and cast bushes. Wear is investigated by comparing the morphology of specimens obtained from different parts of the same bearing that have undergone different levels of wear.

The results obtained provide further elements, in addition to the more standard macro-tribological characterization, for the choice of the material of best performance. In particular, electroplated bushes have been confirmed to exhibit the best tribological behaviour since their sliding friction coefficient is lower than the one measured on the cast bush.

Parole chiave: rame e leghe, elettrochimica, rivestimenti, tribologia, selezione materiali

INTRODUCTION

The tribological characteristics of coatings are very important for journal bearings designed for severe working conditions. In particular in boundary lubrication conditions, some contacts between asperities can occur and microscopic aspects become of importance. An investigation at the micro-nanometric scale is therefore useful.

To this aim, peculiar kinds of microscopes sensitive to mechanical properties down to the nanometer scale must be used, namely, scanning force microscopes (SFM). In particular, the contact mode atomic force microscope (AFM) is the more suitable for the study of morphology and tribological effects on the micro-nanometer scale [1]. Such technique is customarily employed for the characterization of solid thin films [2] and is able to provide absolute values of the local kinetic, or sliding, friction [3]. Specifically to the present study, AFM provides tribological information of two kinds, namely, about the morphology and the kinetic friction at the micro-nanometer scale, evidenced when the sharp probe of an AFM, supported on an elastic cantilever beam, is moved laterally while contacting the sample surface. Such technique, named friction force microscopy (FFM) [4], is accomplished in a standard AFM by detecting the twisting movement of the cantilever beam due to the lateral force acting on the tip, and provides information on the amount of sliding friction between the AFM tip and a local portion of the sample surface.

In the atomic force microscope, a raster scan of the sample on the X-Y plane (Fig. 1) is realized by means of piezoelectric transducers with a precision in the range of the angstrom. The raster scan is performed with a nearly uniform motion in the X direction, with a trace movement and a subsequent retrace over the same scan line. After the retrace, a step is made in the Y direction and the cycle is repeated to complete the raster. Thus, the tip motion that generates friction is always the one on a definite direction, referred to as fast scan (X) direction.

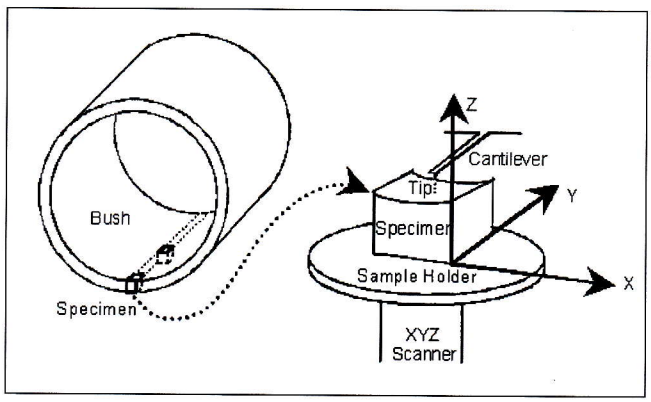

Fig. 1. Sketch of the bush (left) from which the small specimens are cut and transferred to the AFM scanner (right). The tip is approached to the surface with the geometry shown on the sketch. Proportions are not respected in the drawing.

Fig. 1. Disegno schematico della boccola (a sinistra) da cui sono stati ricavati i piccoli provini usati per le prove con l'AFM. Nello schema a destra è mostrata la geometria del sistema con cui la punta dell'AFM è accostata alla superficie del provino (il disegno non è in scala).

The fast scan direction must be perpendicular to the longitudinal axis of the cantilever beam, to maximize the torque caused by the lateral force on the beam, and thus the sensitivity of the friction measurement. Was the fast motion performed parallel to the longitudinal axis, the friction force would have no lateral component and the twisting movement generated would be null. This implies that, in order to obtain the friction coefficient due to sliding at different directions on the surface, the sample must be physically rotated with respect to the cantilever, since the simple scan direction rotation would also affect the sensitivity of the FFM as mentioned above. For instance, in the case of the bearings considered in the present study (Fig. 1), the samples have been oriented with the bush longitudinal axis nearly parallel to the cantilever longitudinal axis. In such way the sliding motion realized in the AFM will be in the same direction than for the bearings in operation. We have indeed concentrated on the friction recorded in such direction since it is

R. Bassani, E. Ciulli
Dipartimento di Ingegneria Meccanica, Nucleare e della Produzione, Università di Pisa

M. Labardi, M. Allegrini
INFM and Dipartimento di Fisica, Università di Pisa

Paper presented at the 7th European Conference EUROMAT 2001, Rimini 10-14 June 2001, organised by AIM

more meaningful for comparison with data on macroscopic friction. The AFM topographic image, on the contrary, provides exclusively geometrical information, and the result is nearly independent on the mutual orientation between cantilever and sample.

For FFM measurements the AFM is operated in the so-called constant force mode, that ensures a more meaningful interpretation of the measured friction in terms of an average friction coefficient. In this mode, customarily employed in AFM, the force exerted by the elastic cantilever on the tip that contacts the sample is held constant. This is realized by adjusting the sample position in the Z direction, that is orthogonal to the raster scan plane and nearly parallel to the direction of the interaction between tip and sample. In such a way, the normal deflection of the cantilever is maintained to a constant value. Such deflection is proportional to the external force exerted on the tip, namely the elastic force, that our system holds constant regardless of the topography encountered during the scan. With no such adjustment, for instance, topographic reliefs would act to bend the cantilever backwards and to increase the exerted force, and vice versa for topographic valleys. The Z adjustment is performed in AFM by the same piezoelectric transducer that actuates the raster scan.

In the present study, different parts of a couple of bearings are investigated, that have undergone different levels of wear, by comparing the morphology of specimens obtained from the two bushes. These are a cast and a electroplated bush that have worked in extreme conditions. One method used for wear investigation is to compare the morphology (general appearance and roughness) of the specimens, included the case of heavy and low wear. With the same positioning accuracy, it has been also possible to measure the friction force on the sub-micrometer scale, to reveal local variations of the friction coefficient, on the same areas examined by topography inspection, that have undergone different wear phenomena. Investigation of the friction of dry surfaces can provide for instance peculiar information as regards extreme working conditions of the bearings, e.g., due to the interruption of lubricant supply. Similar studies can be performed on lubricated surfaces; this is the subject of a future work.

MATERIALS AND METHODS

A couple of lead bronze coatings of advanced type, particularly suitable for journal bearings, have been investigated. One has been electrodeposited (with a thickness of about 40 μm) and the other one has been melded (for a thickness of about 0.8 mm) on a steel base. Therefore the coating type will be identified by referring to "electroplated" (E) and "cast" (C) bushes. On the electroplated bush a very thin layer of lead is also deposited. All bearings have been provided by FiatAvio [5].

Parts of the two bushes that have undergone different levels of wear in extreme working conditions are shown in Fig. 2. In Fig. 2 images are reported with the indication of the five different combinations of coating type and wear degree considered in this study (the same labels are cited in the tables reported below). It is interesting to note that the layer of lead was removed in the zone E_H.

Specimens of typical area between 0.25 and 1 cm^2 are cut from the regions of the two bushes that have undergone different amounts of wear. A summary of the different specimens used is given in Table 1. For each of the five cases considered, given by the combination of coating type and wear degree, a couple of different points have been chosen to carry out measurements for our tribological and morphological investigation.

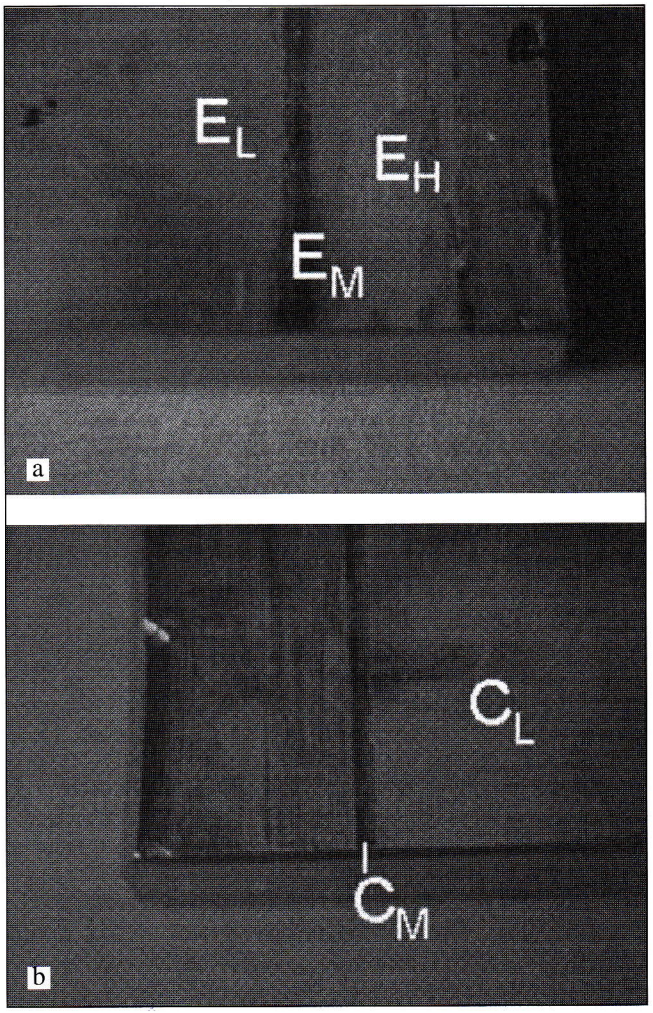

Fig. 2. Optical microscope images (30 x 20 mm^2) of portions of electroplated (a) and cast (b) bushes. The investigated zones with different wear degree are characterized by the different labels.

Fig. 2. Immagini (30 x 20 mm^2) ottenute con microscopio ottico di parti di superfici di boccole con riporto elettrodepositato (a) e fuso (b). Le diverse lettere individuano le zone analizzate che presentano diverso livello di usura.

Specimen	Coating type	Wear degree	Zone (Label)
E1	Electroplated	Low (zero)	E_L
E1	Electroplated	Medium	E_M
E2	Electroplated	Heavy	E_H
C1	Cast	Low (zero)	C_L
C1	Cast	Medium	C_M

Table 1. Specimens investigated by AFM/FFM. The labels are identifiers for the coating type and wear degree (used in the following section).

Tabella 1. Provini analizzati con AFM/FFM. Le etichette usate individuano sia il tipo di rivestimento (E: elettrodepositato, C: fuso) sia il livello di usura (L: basso, M: medio, H: alto).

The instrument used for the measurements is a home-made AFM/FFM head [6] operated in air at room temperature, interfaced to a commercial Burleigh controller [7]. The AFM sensors adopted are boron-doped silicon AFM cantilevers of contact mode type (nominal tip radius 5 – 10 nm), from Nanosensors [8]. The bending and twisting spring constants of the cantilever have been determined by standard procedures (Ref. [1], p. 193). Magnified images of the cantilever have been obtained by a Nomarski microscope, and the actual

length l and width w have been measured. Thickness t has been determined by measuring the fundamental resonance frequency f of the cantilever. The obtained values are f = 13 kHz, t = 1.9 μm, l = 443 μm, w = 55.5 μm. The tip height h has been assumed as the average of the values declared by the manufacturer (10-15 μm). All this leads to a bending spring constant of 0.17 N/m and a torsional spring constant of 0.94 10^{-3} N/rad. Force vs. separation curves (reported below) have been used for assessing the absolute normal force calibration of the AFM, that resulted 75% higher than estimated. Unfortunately, the same refinement cannot be done for the lateral force, that is therefore affected by a possible tolerance.
The surface of the dry specimens has been washed with acetone and rinsed with ethanol prior to AFM measurements. Special test measurements, made on purpose both in Argon flux atmosphere and in ambient, provided no evidence of the effect of atmospheric contaminants on the measured friction. Thus, all measurements have been performed in air.
Measurements are typically conducted as follows. The specimen is attached to the piezoelectric scanner (Fig. 1) by means of adhesive tape. An electrical connection is made between the cantilever and the sample, in order to eliminate fluctuating electrostatic forces that are detrimental to the absolute measurement and control of normal forces. The tip is approached to the sample surface and a force versus separation (FS) curve is acquired, that is, the sample Z position is changed linearly and the corresponding cantilever deflection is recorded. For the description of such a curve let us refer to Fig. 3. It is well known from the basics of AFM that in the approach stage the cantilever sticks to the surface with the so-called jump-in-contact (JIC) phenomenon. In the graphs of Fig. 3, such point is set as the zero of the sample position. Further approaching leads to an elastic regime where the cantilever bending equals the Z movement of the sample, while the load increases. Upon withdrawing the sample, the JIC point is surpassed and the tip detaches from the surface at the jump-off-contact (JOC) point.
Such hysteretical behaviour can be described in terms of the bistability of the solutions of the equation of motion of the system

$$F_{int} + F_{el} = 0 \qquad (1)$$

Here F_{int} represents the tip/sample interaction force, roughly depictable as a force derived from a Lennard-Jones type potential, and F_{el} is the elastic force due to the cantilever bending, that is, what we will call the (imposed) normal load. When the stiffness k of the cantilever is exceeded by dF_{int}/dz at some distance z_{JIC}, the cantilever sticks in contact, that is, jumps from one solution to the other, at a position slightly closer to the surface, where the sign of dF_{int}/dz is negative. On withdrawing, a different jump happens at the distance z_{JOC}, where the interaction exhibits about the maximum attractive character, to a much farther z value. Such jumps can be avoided by using very stiff cantilevers, that on the other hand show decreased sensitivity in the contact mode, and must be used at higher force set values with deleterious effects on both tip and sample surface. The value of the jump-off (or pull-off) force carried out from the FS curve provides the strength of the attractive interaction between the two materials composing the tip as well as the sample region where the tip has contacted. Variability of such force may indicate local differences in composition of the surface [9]. After recording the FS curve, raster scans over an area of 1.25 x 1.25 μm^2, made up by 128 scan lines (trace plus retrace) are made, for several values of the loading force. At each investigated point, a series of friction measurements at different loads has been carried out to compose a friction plot, from which the friction coefficient is carried out by a linear fitting (Fig. 4). Each measurement series is identified by a letter (appearing on Table 3 in the Results and Discussion section)

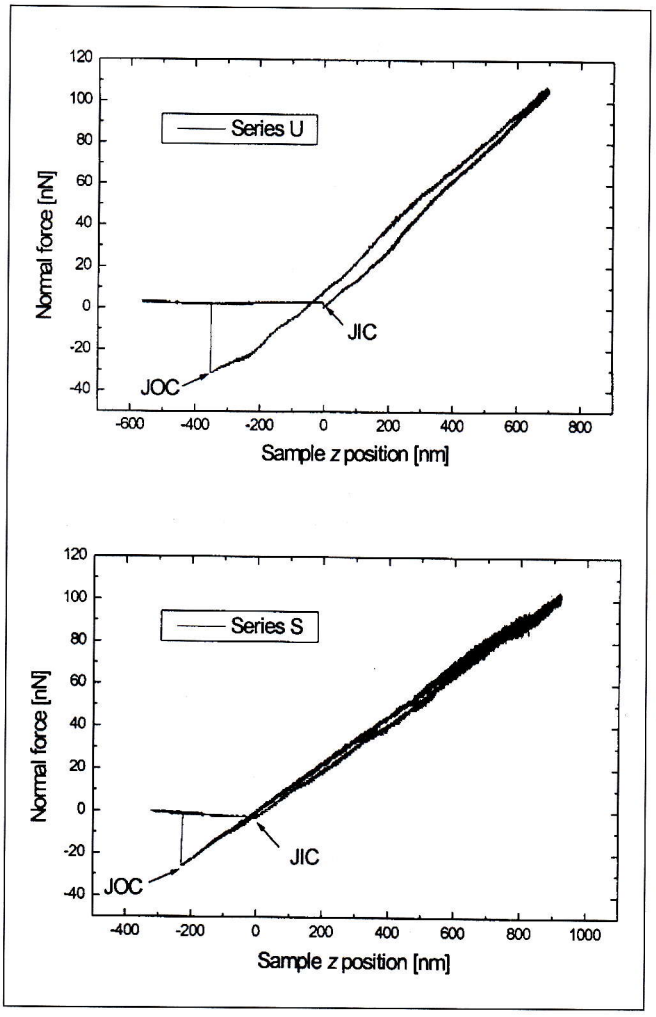

Fig. 3. Examples of force versus separation (FS) curves. Series U refers to zone E_M, S to zone C_L.

Fig. 3. Esempi di curve forza-separazione (FS). La serie U si riferisce alla zona E_M, la S alla C_L.

so that the alphabetical order provides the temporal sequence of the measurements made.
The friction measurements have been carried out as follows. Since our commercial AFM system [7] does not support the simultaneous trace and retrace image acquisition, compulsory for the usual friction evaluation based on statistical analysis of the friction images acquired in opposite directions [3], an additional acquisition system has been set up. Such system computes automatically the average friction force value on the full raster scan, by carrying out the line integral of the friction force on the fast scan direction, for each raster line, and eventually averaging the result on the 128 lines comprising the raster. Such average value expressed in nN is plotted versus the set elastic force, maintained constant on the entire scan, on friction plots as the ones shown in Fig. 4.
The kinetic friction coefficient m is defined by the law:

$$F_f(F_{el}) = F_f(0) + \mu F_{el} \qquad (2).$$

A linear fit provides the average friction coefficient on the scanned area of 1.25 x 1.25 μm^2, as well as other characteristic forces, like:

1) $F_f(0)$, the friction force at zero load, carried out from the fitting of the friction plot and thus to be considered as an average value on the scanned area, corresponding to the friction between tip and sample where the exerted force is only due to their mutual interaction, that is, when the mutual distance corresponds to the equilibrium one between

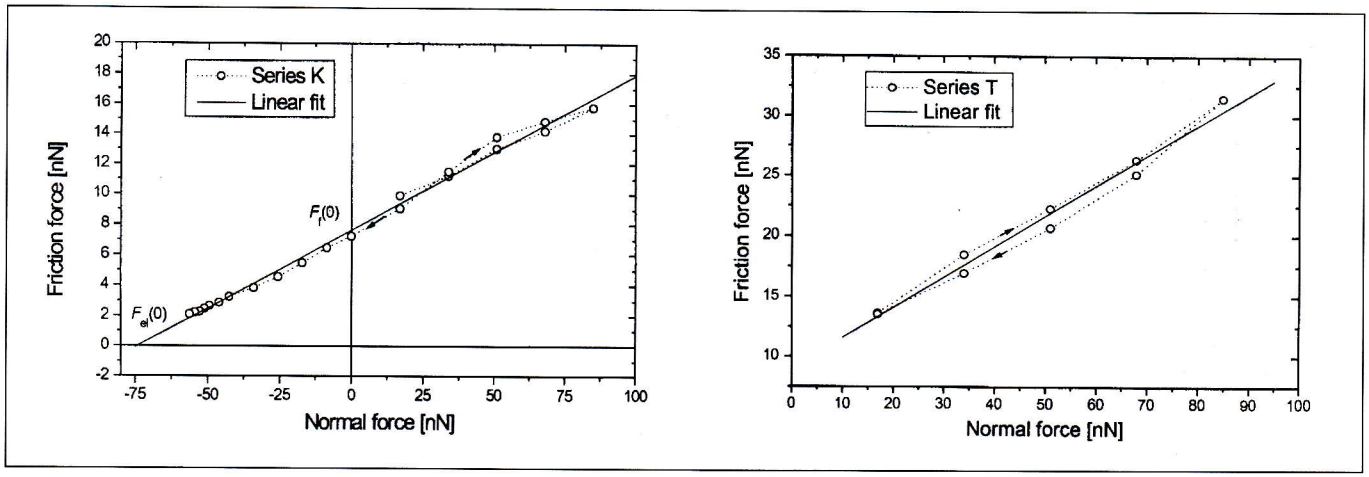

Fig. 4. Examples of friction plots. The fitting provides values for the average friction coefficient μ, the friction force at zero load $F_f(0)$, and the normal load for zero friction $F_{el}(0)$. The arrows indicate the temporal sequence of the friction measurements.

Fig. 4. Esempi di diagrammi di attrito. La retta di regressione permette di valutare il coefficiente d'attrito μ, la forza d'attrito a carico nullo $F_f(0)$, ed il carico normale a cui corrisponde attrito nullo $F_{el}(0)$. Le frecce indicano la successione temporale delle misure d'attrito.

Type of sample area	Series	m	$F_f(0)$ [nN] (from fit)	$F_{el}(0)$[nN] (from fit)	F_{JOC} [nN] (FS curve)
Electroplated, low wear	J	0.10	6.7	-66	-46
E_L	K	0.10	7.6	-74	-46
Electroplated, medium wear					
E_M	G	0.10	5.6	-55	-68
	U	0.13	4.4	-33	-31
Electroplated, heavy wear	L	0.11	3.2	-29	--
E_H	N	0.27	6.7	-25	-36
Cast, low wear					
C_L	S	0.24	4.4	-18	-26
	T	0.25	9.0	-36	-11
Cast, medium wear	O (*)	0.34	6.6	-19	0
C_M	R	0.27	7.5	-28	-19
Silicon, monocrystalline	Q	0.19	37	-185	-148

Table 2. Summary of the experimental results. m indicates the average kinetic friction coefficient, obtained by linear fitting of the friction force at different load values. $F_f(0)$ is the friction force, expressed in nN, at zero elastic force, carried out from the same fitting that provides the friction coefficient. $F_{el}(0)$ is the elastic force, carried out from fitting, at which zero friction force is extrapolated. The last column reports the values of F_{JOC} carried out from the analysis of force/separation (FS) curves. The (*) indicates series taken on a sample not previously cleaned, with possible presence of lubricant residuals.

Tabella 2. Sintesi dei risultati sperimentali. m indica il coefficiente d'attrito cinetico medio, ottenuto per regressione lineare dei valori della forza d'attrito ai diversi valori di carico. $F_f(0)$ è la forza d'attrito, espressa in nN, misurata per forza elastica nulla, ottenuta dalla stessa regressione usata per il coefficiente d'attrito. $F_{el}(0)$ è la forza elastica, estrapolata usando la stessa regressione, a cui corrisponde un valore nullo della forza d'attrito. L'ultima colonna riporta i valori di F_{JOC} ricavati dalle curve forza-separazione (FS). L'asterisco indica serie ottenute con un campione che non ha subito il trattamento di pulizia superficiale prima delle misure, quindi con possibile presenza di residui di lubrificante.

the atoms of the two materials.

2) $F_{el}(0)$, the normal load that provides zero friction force, carried out from the fitting of the friction plot and thus to be considered as the average value of the pull-off force on the scanned area; this value is also to be assumed as the zero of the actual load of the tip/sample junction [10];

Another quantity of interest, carried out from our measurements is referred to as F_{JOC} (FS curve). It is the pull-off force determined by the force/separation curve, that is taken at one single position of the surface, and thus is not expected to be equal to the average pull-off force on the scanned area, since it refers to the particular interaction at the position of the approach.

After the friction measurements, a zoom-out 12.5 x 12.5 μm^2 AFM topographic image, followed by a further 33 x 33 μm^2 zoom-out image, have been recorded. The absolute velocity of sliding has been maintained constant for all the measurements, included the large scale topographies, to about 10 μm/s. The range of elastic forces (normal loads) used for the friction measurements spans from –170 to +85 nN. Topographic images at lower magnification are typically taken at a normal load of 17 to 34 nN.

RESULTS AND DISCUSSION

A summary of the friction results obtained in different points of the specimens is reported in Table 2. It is interesting to note how F_{JOC} is influenced by the materials: its value for the contact between silicon (the tip material) and lead (the electroplated bush material) is about twice the one between silicon and bronze (the cast bush material). Mean

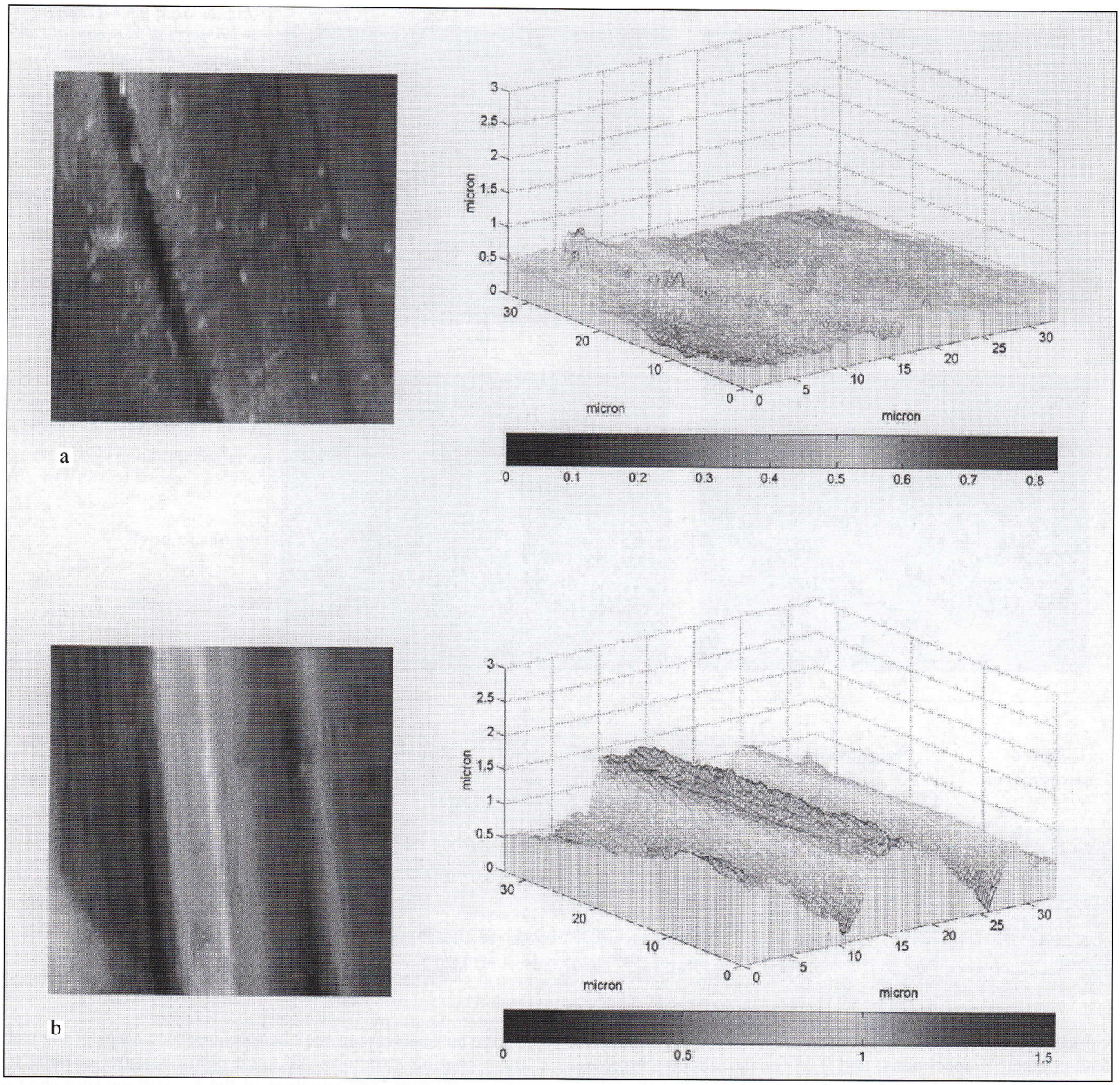

Fig. 6. AFM top view images and corresponding 3D plots for low wear zones. (a) E_L, series K, (b) C_L, series T. Higher points are shown by bright grey tones on the AFM images. The origin of the 3D reference frame corresponds to the left bottom corner of the AFM image.

Fig. 6. Immagini AFM e corrispondenti grafici tridimensionali ottenute in zone con bassa usura. (a) E_L, serie K, (b) C_L, serie T. Le zone più chiare sulle immagini AFM corrispondono alle asperità più alte. Le origini dei grafici tridimensionali corrispondono agli angoli in basso a sinistra delle immagini AFM.

μm^2 AFM topographic images. The average roughness is strictly dependent on the area considered; this point is fundamental for comparison with values carried out by conventional stylus profilometry, that traces profiles of a few millimeters length.

Just to give a hint, mean values for macroscopic roughness of the bushing surfaces before running were Ra = 0.25-0.75 µm for the electroplated bush and Ra = 0.45 µm for the cast bush.

It is also evident that the roughness values determined by AFM are in general lower for the smaller areas except for some cases when tracks are located within the scanned area. A sort of running-in can be supposed comparing value of roughness for low and medium wear, both for electroplated and cast bushes. However, some deep tracks are present in some E_M zones.

CONCLUSIONS

Two kinds of bushes for journal bearings, an electroplated and a cast one, that have worked in extreme lubrication condition have been investigated by atomic and friction force microscopy. The bushes have undergone different levels of wear. Topographic investigations as well as friction measurements have been made that show the influence of the different materials on morphology as well on tribological behaviour. The electroplated bush seems to present a lower surface roughness in comparison with the cast one even in presence of wear. This has been proven by the topographic AFM investigation as well as by the images obtained by SEM. This best tribological behaviour of the electroplated bush is also confirmed by the friction measurements made by the AFM.

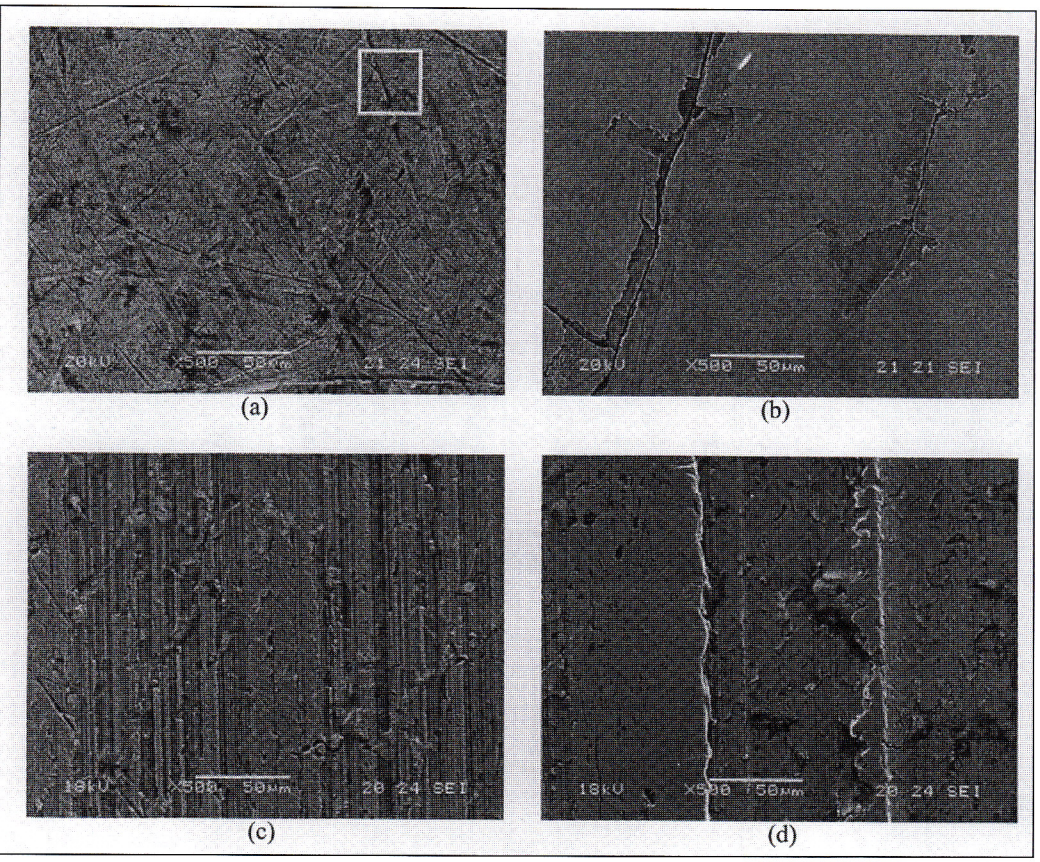

Fig. 5. SEM micrograph (250 x 190 μm²) of a region of type E_L (a), E_H (b), C_L (c) and C_M (d). The white square in (a) represents the relative size of the 33 x 33 μm² area of our AFM images.

Fig. 5. Immagini SEM (250 x 190 μm²) di zone di tipo E_L (a), E_H (b), C_L (c) e C_M (d). Il riquadro bianco in (a) corrisponde alla tipica superficie di 33 x 33 μm² investigata con l'AFM.

Type of sample area	Height range [μm]		Roughness R_a [μm]		Roughness R_q [μm]	
	33x33	12.5x12.5	33x33	12.5x12.5	33x33	12.5x12.5
E_L	0.8	0.7-0.9	0.07	0.055-0.075	0.095	0.105-0.11
E_M	0.7-2.5	0.5-1	0.05-0.055	0.04-0.045	0.07-0.155	0.06-0.07
E_H	1.1	0.5	0.10	0.06	0.12	0.08
C_L	1.5-2.1	0.5-1.1	0.22-0.30	0.085-0.215	0.27-0.35	0.095-0.24
C_M	1.0-1.6	0.7-0.8	0.115-0.16	0.07-0.09	0.15-0.2	0.095-0.11

Table 3. Roughness extracted from the AFM topographic data of an area 33 x 33 μm² and 12.5 x 12.5 μm².

Tabella 3. Valori di rugosità ricavati dalle analisi topografiche effettuate con l'AFM su superfici di 33 x 33 μm² e 12.5 x 12.5 μm².

values of the friction coefficient m are 0.11 for the silicon - lead contact (E specimens) and 0.25 for the silicon - bronze contact (C specimen and parts of the E_H zone). For the silicon - silicon contact, reported for comparison and also interesting for electronic applications, μ is around 0.19. It is to be noted that these values are of the same order of magnitude than the ones obtained for the corresponding contacts at macroscopic level.

For the explored force regime, giving rise to a point contact pressure of the order of 1 GPa, values of the friction coefficient for the silicon – silicon sliding contacts from 0.03 to 0.11 are reported in the literature [11, 12]. This could be the hint of an overestimation of the lateral force due to well-known tolerances in their calibration procedure [3, 11]. However, the friction force and friction coefficient relative comparison remains fully meaningful.

The increase of the friction coefficient by increasing wear does not seem significative. Actually, the areas of 1.25 x 1.25 μm² have been chosen in order to limit the number of asperities on the scanned surface. At this microscopic level interatomic forces and therefore material coupling are predominant. However, a different surface roughness has been measured for the different wear and material combinations in the 12.5 x 12.5 μm² and 33 x 33 μm² areas concerned by topographic investigation. The SEM images reported in Fig. 5 give an overview of the electroplated as well as of the cast bush coating structure. All such pictures show an area of 250 x 190 μm². The situation of the E_M surface (not shown in Fig. 5) is similar to the one of E_L, apart from a reduction of the number of tracks, probably related to a sort of running-in effect. Zones with and without the lead coating can be noticed in Fig. 5b; this explains the different results obtained for m for the two series L and N.

In Fig. 5a the dimension of a square of 33 x 33 μm² is also reported to show the relative size of the AFM images reported below.

Fig. 6 shows a top view AFM comparison between a typical area for medium wear regions of both kinds of bushes (E_L and C_L). AFM measurements provide calibrated height maps, so that it is easy to obtain 3D picture of the scanned surfaces as shown in the figure.

The electroplated bush seems to present the best morphology. The improved behaviour of this kind of coating in comparison with the cast one has been proven also through an investigation made by an optical microscope (images not reported). Fig. 7 shows the morphology of the surface in a region of the worn zone E_H where some lead is still present.

The average roughness of the surface can be obtained as well by the AFM investigation. Table 3 resumes the roughness values carried out from the 33 x 33 μm² and 12.5 x 12.5

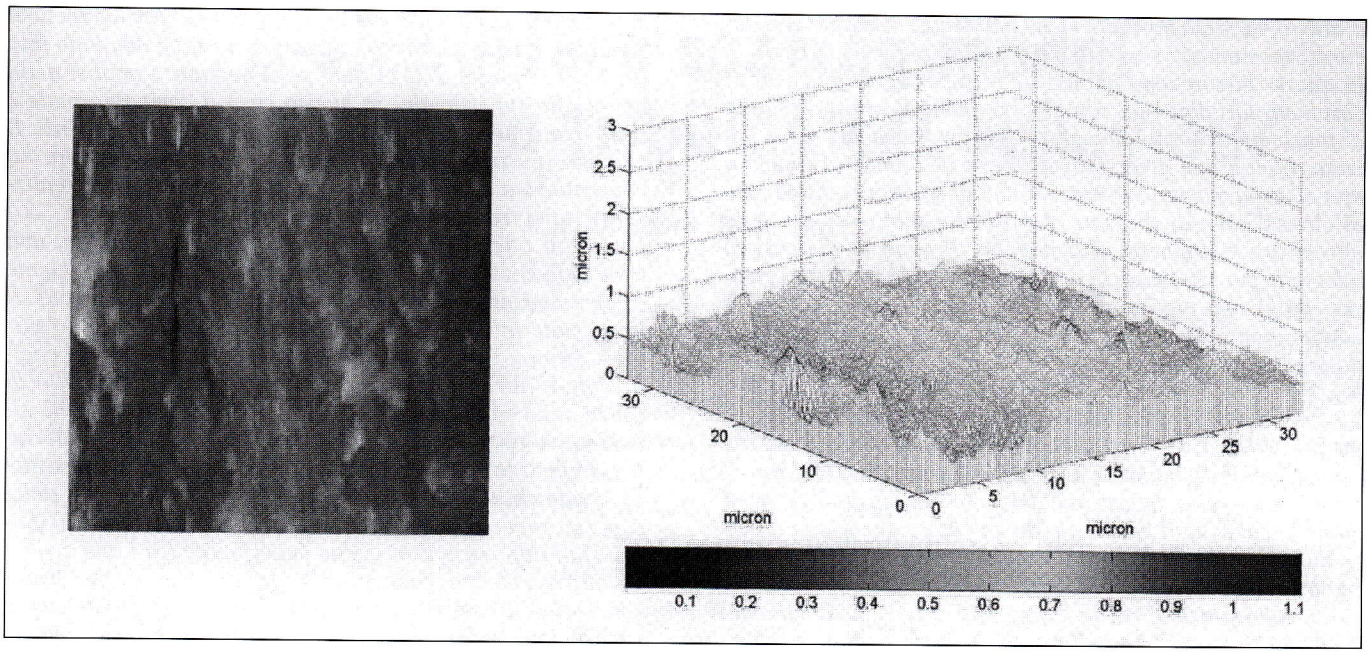

Fig. 7. AFM images and corresponding 3D surfaces for wear zone E_H, series L.

Fig. 7. Immagini AFM e corrispondenti grafici tridimensionali ottenute nella zona ad alta usura E_H, serie L.

ACKNOWLEDGEMENTS

The authors wish to thank G. Barattini for carrying out some of the tests, P. Narducci for the SEM images, L. Pardi for the realization of the X-Y micrometer stage for the AFM coarse sample positioning.

REFERENCES

1) B. BHUSHAN Ed., Micro/Nanotribology and its applications, NATO-ASI Series E: Applied Science 330, Kluwer Academic Publishers, Dordrecht (1997).
2) M. LABARDI, M. ALLEGRINI, F. LECCABUE, B.E. WATTS, C. ASCOLI and C. FREDIANI, Sol. St. Commun. 91, (1994), p.59.
3) M. LABARDI, M. ALLEGRINI, M. SALERNO, C. FREDIANI and C. ASCOLI, Appl. Phys. A 59, (1994), p.3.
4) C.M. MATE, G.M. MCCLELLAND, R. ERLANDSSON and S. CHIANG, Phys. Rev. Lett. 59, (1987), p.1942.
5) R. BASSANI, B. PICCIGALLO, E. CIULLI and G. ODDONE, Proc. 2000 AIMETA Int.Tribology Conference, L'Aquila (2000), Gruppo Tipografico Editoriale, L'Aquila (2000), p.347.
6) M. LABARDI, M. ALLEGRINI, E. MARCHETTI and P. SGARZI, J. Vac. Sci. Technol. B 14, (1996), p.1509.
7) Burleigh Instruments Inc. Metris-2000 AFM controller (Fishers, NY, USA, 1997) with Advanced True Image Software, Cavendish Instruments Ltd. (Sheffield, UK, 1999).
8) Nanosensors GmbH, Wetzlar-Blankenfeld, Germany.
9) T. STIFTER, E. WIELANDT, O. MARTI and S. HILD, Appl. Phys. A 66, (1998), p. S597.
10) O. ZWÖRNER, H. HÖLSCHER, U.D. SCHWARZ and R. WIESENDANGER, Appl. Phys. A 66, (1998), p. S263.
11) BHUSHAN, Principles and Applications of Tribology, John Wiley & Sons, Inc., New York (1999).
12) S. NIEDERBERGER, H.H. GRACIAS, K. KOMVOPOLOUS and G.A. SOMORJAI, J. Appl. Phys. 87, (2000), p. 3143.

ABSTRACT

ANALISI DELL'USURA DI RIVESTIMENTI PER CUSCINETTI PORTANTI MEDIANTE MICROSCOPIA A FORZA ATOMICA

Le caratteristiche tribologiche dei rivestimenti per cuscinetti portanti sono di grande importanza soprattutto nel caso che siano progettati per funzionare in condizioni gravose (ad esempio carichi altissimi, velocità basse o molto elevate, scarsa alimentazione di lubrificante). In particolare quando si raggiungono condizioni di lubrificazione limite con contatti diretti fra le asperità superficiali dei due elementi accoppiati, gli aspetti microscopici diventano importantissimi. Indagini micro- e nanometriche sulle superfici possono essere effettuate con particolari tipi di microscopi che consentono di indagare fino a livello molecolare e atomico. Fra di essi il recente microscopio a forza atomica (AFM) usato in modalità di contatto è il più adatto per studiare la morfologia e l'attrito fino ad una scala micro/nanometrica. Nell'AFM usato in questo lavoro, realizzato presso l'INFM e il Dipartimento di Fisica dell'Università di Pisa, una piccolissima punta di silicio, sostenuta da un sottile supporto elastico, viene posta a contatto con la superficie del campione da analizzare; quest'ultimo viene mosso da un trasduttore piezoelettrico in modo tale da investigare la superficie per linee parallele. Dalla torsione del supporto elastico, misurata grazie alla riflessione di un raggio laser su di essa inviato e rilevato da un sensore a quattro quadranti, si risale sia alla topografia superficiale sia alla forza d'attrito sviluppata nel contatto fra punta e superficie. Per le misure della forza

d'attrito, la forza normale viene mantenuta costante con accurati spostamenti verticali del trasduttore piezoelettrico.
In questo lavoro sono analizzate le superfici di due sedi di cuscinetti idrodinamici con diversi livelli di usura a seguito di funzionamento in condizioni gravose. Le boccole, in acciaio, hanno due diversi rivestimenti di bronzo al piombo: uno elettrodepositato di circa 40μm di spessore ed uno fuso di circa 0.8mm di spessore. La prima è inoltre rivestita da uno strato micrometrico di piombo. Provini di dimensioni adeguate per effettuare le misure con l'AFM sono stati ricavati dalle boccole e detersi per eliminare ogni traccia di contaminanti. Su ogni provino sono state individuate zone da analizzare con diverso grado di usura (basso, medio, alto). Per ogni zona superficiale di provino investigata l'origine della posizione verticale è stata stimata preliminarmente mediante le curve forza-separazione ottenute accostando e allontanando la punta dell'AFM dalla superficie del provino e rilevando la deflessione del supporto elastico: la posizione in cui si ha il passaggio da un valore di carico normale nullo ad un andamento crescente linearmente, chiamato punto di salto in contatto (JIC), è stata presa come zero dello spostamento. Ritraendo la punta, si evidenzia un fenomeno di adesione tra le superfici con la presenza di un punto di salto fuori contatto (JOC) a forza applicata dal supporto elastico negativa. Superfici di 1.25x1.25μm² sono state analizzate secondo 128 linee parallele percorse nei due sensi con velocità costante di 10μm/s. I valori di forza d'attrito misurati per diversi valori di carico normale (da –170 ad +85nN) hanno presentato andamenti quasi lineari in funzione di quest'ultima grandezza; dalle rette di regressione ottenute è stato quindi ricavato il coefficiente d'attrito cinetico. Successivamente le zone analizzate sono state ampliate fino a 12.5x12.5μm² e a 33x33μm² per effettuare l'analisi della topografia superficiale; in questo caso il carico normale è stato mantenuto a valori costanti compresi fra 17 e 34nN. Il software utilizzato, in parte appositamente realizzato, ha consentito sia di ricavare tutti i dati di rugosità sia di realizzare grafici tridimensionali delle superfici.
I risultati ottenuti hanno mostrato, come prevedibile, una forte influenza del materiale. In particolare il coefficiente d'attrito misurato è stato circa 0.11 per l'accoppiamento silicio (materiale della punta) – piombo e 0.25 per quello silicio – bronzo. Un certo limitato aumento del valore del coefficiente d'attrito è stato rilevato al crescere del livello di usura della superficie analizzata, ma sicuramente meno significativo rispetto a quello legato all'influenza del materiale (in effetti le zone analizzate sono state volutamente scelte estremamente piccole in modo da limitare l'effetto delle asperità superficiali nelle prove per le misure d'attrito). Sostanziali differenze di rugosità superficiale fra i due diversi tipi di rivestimento come pure fra le zone con diversa usura sono state invece riscontrate con le analisi effettuate con le superfici più grandi. Tali differenze sono state anche confermate da un'indagine effettuata sugli stessi provini con un microscopio ottico e con un microscopio elettronico. I valori di rugosità ottenuti confermano la loro nota dipendenza dall'ampiezza della zona di superficie investigata. In ogni caso la boccola elettrodepositata sembra possedere una migliore morfologia superficiale rispetto alla boccola fusa, presentando valori di rugosità inferiori anche nelle zone usurate.